The muon – a probe for Condensed matter

W.E. Fischer
Paul Scherrer Institut, CH-5232 Villigen PSI

The muon – a probe for Condensed matter

I. The Muon and its production as an elementary particle [1]

According to present wisdom the muon is an elementary particle. Together with its neutrino it represents the leptonic part of the second generation (out of three generations). It is the equivalent of the electron, which belongs to the first generation. Theses particles appear in the elementary scheme as indicated in fig. 1. While the electron is stable, the muon decays through a weak interaction process. Apart from its bigger mass, the properties of the muon are however identical to those of the electron. But unlike the electron, since muons are unstable, they have to be produced in high energy reactions. The most abundant reaction channels for muon production lead through the production and decay of pions. The corresponding reaction chain takes place in the upper atmosphere of the earth, caused by cosmic rays or on laboratory targets, bombarded by high energy protons.

With a proton beam higher energy (E>180 MeV) onto a target of any kind the following reactions may proceed:

$$p + n \rightarrow n + n + \pi^{+} \tag{1.1}$$

$$p + p \rightarrow p + n + \pi^{+} \tag{1.2}$$

$$p + n \rightarrow p + p + \pi^{-} \tag{1.3}$$

There exists also neutral pion π^0, which may be produced in a similar manner.

$\pi^{\pm}$-mesons are strongly interacting particles with a mass of 139.6 MeV, which decay via weak interaction with a mean lifetime of $2.6 \cdot 10^{-8}$s. These mesons are pseudo-scalar particles with spin and parity 0^-. Among the various possible decay channels a particular one dominates all the others. More then 99.9 % of the $\pi^{\pm}$-mesons decay through

$$\boxed{\pi^{+} \rightarrow \mu^{+} + \nu_{\mu}} \tag{1.4}$$

into muons and muonic neutrinos, both possessing a spin of $1/2$. As mass less (or nearly so) Dirac-particles the neutrino is of left handed chirality (respectively right handed for the antineutrino). Due to momentum conservation the decay geometry is collinear. In order to keep angular momentum conserved the decay lepton has to carry its spin opposite to the one of the neutrino. This decay configuration is shown for the $\pi^{+}(0^{-})$-decay in Fig. 2. For a mass less lepton this configuration would be forbidden. That is, why the decay channel $\pi^{+} \rightarrow e^{+} + \nu_{e}$ is – due to the much smaller mass of the positron – highly suppressed ($<10^{-4}$) in spite of the much larger phase space available.

We recognize that a muon beam produced by means of π-decay should always be highly polarized. The following two situations are typical:

- Pion decay in flight
  The corresponding muons have an energy of 40-50 MeV and a polarization $P \cong$ 60-80%. About 15 g/cm^2 of material is needed to degrade the kinetic energy of the muons. A rather homogeneous stop throughout the sample can be achieved – a quite adequate condition for investigation of bulk properties of the sample.

- Surface beam
  Pion decay takes place within or at the surface of the target. Muon energies $\leq$ 4.1 MeV and a polarization of $\cong$ 100% are obtained. The range of these muons is about 170 mg/cm^2, providing good chances for investigating surface properties of the sample.

II. Properties of the muon

The muon has a mass of

m_μ = 105.66 MeV=0.113 m_p = 206.8 m_e.

It can have charge ± e and has spin $1/2$. As already mentioned in the introduction it is elementary and as electron-like Dirac particle has a g-factor near 2; more precisely

g = 2.0023

where the last digits are due to radiative corrections. This leads to a magnetic moment of 3.18 μ_p, which corresponds to a gyromagnetic ratio of

$$\frac{\gamma_\mu}{2\pi} = 13.55 \frac{kH_z}{G} \tag{2.1}$$

The mean of life time is $\tau_\mu = 2.197 \mu s$ with the dominant decay mode

$$\mu^+ \to e^+ + \nu_e + \bar{\nu}_\mu \tag{2.2}$$

$$\mu^- \to e^- + \bar{\nu}_e + \nu_\mu \tag{2.3}$$

This decay is also due to parity violating weak interaction the decay distribution is hence asymmetric – according to Fig. 3

$$\boxed{N_{e^+}(\vartheta) \sim 1 + A\cos\vartheta} \tag{2.4}$$

Here, ϑ is the angle between the muon spin and the momentum of the $e^\pm$.

A = $P \cdot a$, with
- $\cdot P$ as polarization of the muon beam
- $\cdot a$ as asymmetry parameter, defined by the weak interaction mechanism. For detection of all positrons/electrons irrespective of their energy $a = \frac{1}{3}$

The properties of the muons are summarized in table I.

III. Interaction of the Muon with its Environment in a Sample [2]

If a sample is exposed to a muon beam, the muons will be moderated to lower energy through multiple Coulomb scattering and become ultimately thermalized. During this process they keep their polarization. Negative muons will then usually be captured by an atom or a molecule of the sample, forming a so called muonic atom or molecule, where they replace an electron. In spite of the rich physics provided by such systems, we do not consider them any further. We restrict ourself to the case of implantation of positively charged muons. They may come to a halt in an interstitional position and interact with their environments in the lattice in various ways. By means of their charge they may polarize the sample. In isolators or semiconductors the muon may catch an electron into a bound state, forming a hydrogen like atom, the so called muonium. Its hyperfine structure and its distortion by the lattice can serve as a diagnostic tool for the latter. Due to the screening of the charge of the muon by itinerant conduction electrons, muonium seems not to be formed in metals.

In the following we shall concentrate ourself to the case, where a bare μ^+ interacts with his magnetic moment with the local magnetic field.

The corresponding interaction Hamiltonian is

$$H = -\vec{\mu}_\mu \cdot \vec{B}_{\ell oc} = -\gamma_\mu \hbar \vec{S}\vec{B}_{\ell oc} \tag{3.1}$$

where the local field $\vec{B}$ consists of various different contributions as we shall see. The classical equation of motion of the expectation value of the magnetic moment of the muon is then

$$\boxed{\left\langle \dot{\vec{\mu}} \right\rangle = \left\langle \vec{\mu} \right\rangle \wedge \vec{B}_{\ell oc}} \tag{3.2}$$

which describes a precession of the moment around the direction of $B_{\ell oc}$ with a frequency, proportional to the field strength and independent of the angle between $\vec{\mu}$ and $\vec{B}_{\ell oc}$. This is the Larmor frequency

$$\boxed{\omega = \gamma B_{\ell oc}} \tag{3.3}$$

(3.3) tells us that by measuring ω we can determine the local magnetic field within the sample at the location of the mission. This local field consists of a number of contributions; like

- an external field $\vec{B}_{ext}$
- Lorentz field $\vec{B}_L$
- Demagnetization field $\vec{B}_{dem}$

as discussed in classical phenomenology on magnetization. Furthermore – and that is our interest here – we have these interactions of the muon with the electronic degrees of freedom which are also present in absence of an external field. These are

- Dipolar field $\vec{B}_d$ and

- Contact hyperfine interaction $\vec{B}_c$

All this implies that the frequency ω in (3.3) is not the Larmor frequency of the free muon in $\vec{B}_{ext}$ but as already indicated the one which corresponds to the local field $\vec{B}_{\ell oc}$. Furthermore, we recognize that the equation of motion (3.1) is not yet complete. Due to these microscopic interaction the local field is subject to temporal fluctuations, that is

$$\vec{B}_{\ell oc} = \left\langle \vec{B}_{\ell oc} \right\rangle + \delta\vec{B}_{\ell oc} \tag{3.4}$$

where the first term contributes even without an external field if the sample is in an ordered state. The fluctuation term is driving the relaxation of the muon spin ensemble. In order to gather some ideas what we can learn by means of μSR-experiments let us look at the interaction Hamiltonian between the muon and the electrons of the sample.

$$H = -\vec{\mu}_\mu \cdot \vec{B}_{\ell oc} \tag{3.5}$$

where $\vec{B}_{\ell oc}$ - in absence of an external field – is the magnetic field due to the electronic moments. It consists of a dipole – and a hyperfine-interaction. For one electron we have the vector potential

$$\vec{A}_e(\vec{x}) = \frac{\mu_e \wedge \vec{x}}{|\vec{x}|^3} = -\vec{\mu}_e \wedge \vec{\nabla} \frac{1}{|\vec{x}|} \tag{3.6}$$

The magnetic field is then

$$\vec{\nabla} \wedge \vec{\mu}_e \wedge \vec{\nabla} \frac{1}{|\vec{x}|} = \left(\vec{\mu}_e \cdot \vec{\nabla}\right)\vec{\nabla} \frac{1}{|\vec{x}|} + \vec{\mu}_e \Delta \frac{1}{|\vec{x}|} \tag{3.7}$$

For the second term we can write $4\pi\vec{\mu}_e\delta(\vec{x})$, which can be understood as

$$\frac{8\pi}{3} \vec{\mu}_e \eta(\vec{x}) |\psi_e(\vec{x})|^2 \tag{3.8}$$

The factor $\eta(\vec{x})$ introduced here should describe in a phenomenological way the local lattice distortion by the positive muon charge. For many electrons the contributions of (3.7) can be expressed in the following way

$$\sum_i D^{\alpha\beta}\left(\vec{x}_i - \vec{x}_\mu\right) \cdot \mu_e^\beta(\vec{x}_i) + \frac{8\pi}{3} \eta(\vec{x}_\mu) \sum_i H\left(\vec{x}_i \vec{x}_\mu\right) \mu_e^\alpha(\vec{x}_i) \tag{3.9}$$

where

$$D^{\alpha\beta}\left(\vec{x}_i - \vec{x}_\mu\right) = \frac{\delta^{\alpha\beta}}{\left|\vec{x}_i - \vec{x}_\mu\right|^3} - \frac{3\left(x_i - x_\mu\right)^\alpha \left(x_i - x_\mu\right)^\beta}{\left|\vec{x}_i - \vec{x}_\mu\right|^5} \tag{3.10}$$

With $D^{\alpha\beta} = D^{\beta\alpha}$ and $TrD = 0$ clearly expresses the dipole-dipole coupling. H represents an effective exchange coupling of the RKKY-type (Ruderman-Kittel-Kasoya-Ysida [3, 6]). It depends on the

- electron density (localized and unpaired) at the muon site
- exchange interaction of this electron with the conduction electrons
- electron density at the Fermi-surface

This sketch of the interaction of the muon with the electronic environment in the sample may give an idea, how fluctuations of the local field components transverse to the initial polarization cause spin flip transitions and therefore the spin lattice relaxation. The fluctuations reflect the dynamics of the electronic spins at the magnetic atom positions.

Contrary to NMR and Mössbauer spectroscopy the relaxation due to the dipolar field in μSR can be considerable.

IV. The Principle of a μSR-Experiment [2]

Fig. 4 shows the principle of an experimental set up. The polarized muon beam enters the apparatus from the left and triggers in the muon detector a signal to start a clock. After having penetrated the target sample it comes to a rest and precesses there in the local $\vec{B}$-field with its Larmor-frequency. This frequency is determined by

- a possible external field and
- the internal field at the stopping location within the sample.

The decay positron of the muon decay triggers the stop signal for the clock. Due to the precession of the asymmetric decay pattern (2.4) we observe a modulation of the decay law on the positron detector as indicated by the histogram at the lower left of Fig. 4. This counting rate can be parametrized by

$$\frac{dN_e(t)}{dt} = N_0 \frac{1}{\tau_\mu} e^{-t/\tau_\mu} \left(1 + A \frac{\vec{P}(t)\vec{P}(o)}{\left|\vec{P}(o)\right|}\right) \tag{4.1}$$

After transforming away the exponential decay factor of the muon we obtain (lower mid of Fig. 4) what we call the μSR-signal. It shows an attenuated Larmor precession oscillation and is defined by

$$P(t) = \frac{\vec{P}(t)\vec{P}(o)}{\left|\vec{P}(o)\right|^2} = C(t)P(o) \tag{4.2}$$

where the correlation function C is given by the time average

$$\boxed{C(t)=\frac{\left\langle\vec{S}(t)\vec{S}(o)\right\rangle}{S^2(o)}} \tag{4.3}$$

with $\vec{S}$ being the muon spin operator. The Fourier transform of the μSR-signal is shown at the lower right. Note that for different non-equivalent stopping sites of the muon more then one precession line may appear. The attenuation of the μSR-signal is due to polarization relaxing interaction of the magnetic moment with the lattice of the sample.

An essential parameter for μSR-experiments is the external static magnetic field. Various options as part of the set-up are available:

- No external field - $P(t)$ is then solely determined by the internal field
- External field, transverse to $\vec{P}(o)$
- External field, longitudinal to $\vec{P}(o)$

Let $\vartheta =\sphericalangle \left(\vec{B}_{ext}\vec{P}(o)\right)$ be the angle between the external field and the initial polarization. Then in the general case we have

$$\boxed{P(t)=\left|\vec{P}(o)\right|\left[\cos^2\vartheta e^{-t/T_1}+sim^2\vartheta e^{-t/T_2}\cos(\omega t)\right]} \tag{4.4}$$

If $\cos\vartheta=1$ we have the longitudinal case. The relaxation is then described by $\lambda_1 = {}^1\!/_{T_1}$. Since $\vec{P}(o)$ defines the quantization axis of the muon spin, this relaxation is caused by an energy exchange between probe (muon) and sample. This energy exchange has been discussed in the previous chapter as an interaction between the two parts of the total system By its means the probe is driven into thermal equilibrium with the sample within time T_1. The sample hence serves as a heat-bath and T_1 is called spin lattice relaxation.

In the case $\sin\vartheta=1$, no energy is transferred from the muon to the sample. The transverse rate of decay conserves energy in the static field. The decay of polarisation with $\lambda_2 = {}^1\!/_{T_2}$ arises from the spread of precession rates produced by inhomogenity of the local field at the location of the muon. This dephasing is therefore taking place within a time roughly given by $T_2 \sim {}^1\!/_{\gamma B_{eoi}}$.

A few remarks are in order:

1. The result (4.4) is essentially a solution of the semi-classical Bloch equations. The exponential form of relaxation is a very useful postulate to describe most of the phenomena, but must not be taken too literally.

2. For several inequivalent stopping locations i the Fourier-transform of $P(t)$ contains different lines at internal fields $\vec{B}_i$ not necessarily the same in strength and direction at different locations, that is each having its own ϑ_i and Larmor frequency $\omega_\mu^{(i)}$.

Let us finally summarize the parameters to be determined experimentally in a μSR-experiment.

1. The precession frequency ω_μ.

   It differs from the Larmor frequency of a free muon in an external magnetic field (Knight-shift). The difference determines the internal field at the corresponding location.

2. Longitudinal relaxation time T_1

   This is determined by the interaction of the muon with the magnetic degrees of freedom of the sample and their temporal fluctuations.

3. Transverse relaxation time T_2.

   Inhomogeneities of the local magnetic field and their fluctuations are the cause of transverse dephasing of the muon precession and the corresponding depolarization

V. Quantum-mechanical Treatment of the Depolarization Process [3] [4]

The interstitional muon is a two-state system interacting with the environment via the magnetic field. We write for the two eigenstates

$$\left|\frac{1}{2}, m = -\frac{1}{2}\right\rangle \quad and \quad \left|\frac{1}{2}, m = \frac{1}{2}\right\rangle$$

Let their population be N_- and N_+ respectively. We designate the transition probabilities between the two states, which is induced by the fluctuating field in the sample, with W_{-+} and W_{+-}. They are related by

$$W_{+-} = W_{-+} e^{-\hbar\omega/kT} \tag{5.1}$$

where $\hbar\omega$ is the energy split of the two levels and T is the temperature of the sample. For the total numer of muons we write

$$N = N_+ + N_- \tag{5.2}$$

and for the population difference

$$n = N_+ - N_- \tag{5.3}$$

The rate equation for the population is

$$\frac{dN}{dt} = N_- W_{-+} - N_+ W_{+-} = -\frac{dN_-}{dt} \tag{5.4}$$

which can also be written as

$$\frac{dn}{dt} = 2(W_{+-} N_+ - W N_-) \tag{5.5}$$

with $W = W_{-+}$ and reduces to

$$\boxed{\dot{n} = -2Wn} \tag{5.6}$$

if we assume that $\hbar\omega << kT$. Since n is proportional to the polarisation we can put

$$\boxed{\lambda = 2W} \tag{5.7}$$

Hence (5.7) relates the relaxation to the transition rate between the two levels.

We consider now the following Hamiltonian structure for our system:

H_0: unperturbed Hamiltonian of sample and probe; $H_0 = H^{(s)} + H^{(T)}$

H_1: interaction between the two systems; $H_1(t) = -g_\mu \mu \vec{I} \cdot \vec{B}(t)$

$\vec{B}(t)$ is the fluctuating internal magnetic field in the sample. In absence of an external field and at temperatures $(T > T_c)$ above possible ordering we have $\langle \vec{B} \rangle = 0$.

The state population in the sample is assumed to be canonical

$$p_\nu = \frac{1}{Q} e^{-E\nu/kT}; \quad \sum_\nu p_\nu = 1 \tag{5.9}$$

where E_ν are energy eigenvalues of $H^{(S)}$

The transition rate is then (golden rule)

$$W = \lim_{t \to \infty} \frac{1}{t} \frac{1}{\hbar^2} \sum_{\nu,\nu'} p_\nu \left| \langle m'\nu' | \int_0^t H_1(\tau) d\tau | m\nu \rangle \right|^2 = \frac{\lambda}{2} \tag{5.10}$$

In the quantization system of the muon the matrix elements of the angular momentum are

$$\begin{aligned} \langle m' | I_x | m \rangle &= \frac{1}{2} \\ \langle m' | I_y | m \rangle &= -\frac{1}{2} \\ \langle m' | I_3 | m \rangle &= 0 \end{aligned} \tag{5.11}$$

Rotated into the crystal system (see Fig. 5) we obtain

$$
\begin{aligned}
\langle m'|I_a|m\rangle &= \frac{1}{2}\xi(\vartheta,\varphi) &&= \frac{1}{2}(\sin\varphi - i\cos\vartheta\cos\varphi)\\
\langle m'|I_b|m\rangle &= \frac{1}{2}\eta(\vartheta,\varphi) &&= -\frac{1}{2}(\cos\varphi + i\cos\vartheta\sin\varphi)\\
\langle m'|I_c|m\rangle &= \frac{1}{2}\zeta(\vartheta,\varphi) &&= \frac{i}{2}\sin\vartheta
\end{aligned}
\tag{5.12}
$$

From (5.8) we now obtain

$$
\begin{aligned}
&\langle m'\nu'|H_1(t)|m\nu\rangle =\\
&-g_\mu\mu_\mu e^{-i\omega_\mu t}\left\{\xi\langle\nu'|B_a(t)|\nu\rangle + \eta\langle\nu'|B_b(t)|\nu\rangle + \zeta\langle\nu'|B_c(t)|\nu\rangle\right\}
\end{aligned}
\tag{5.13}
$$

with the components of $\vec{B}$ in the crystal system expressed by those in the magnetic system

$$
\begin{aligned}
B_a &= B_x\sin\varphi + B_y\cos\vartheta\cos\varphi &&+B_z\sin\vartheta\cos\varphi\\
B_b &= -B_x\cos\varphi + B_z\cos\vartheta\sin\varphi &&+B_z\sin\vartheta\sin\varphi\\
B_c &= -B_y\sin\vartheta + B_z\cos\vartheta
\end{aligned}
\tag{5.14}
$$

The time dependence of $\vec{B}$ is given by

$$
\vec{B}(t) = e^{-i/tH_0^{(3)}t}\vec{B}(0)e^{i/\hbar H_0^{(3)}t}
\tag{5.15}
$$

Note that (5.15) neglects the influence of the charge of the muon on the sample. In this sense it is an approximation.

Inserting (5.13) into (5.10) we obtain

$$
\boxed{W = \left(\frac{g\mu_\mu}{2\hbar}\right)^2\int_{-\infty}^{+\infty} d\tau e^{-i\omega_\mu\tau}\left\langle\hat{O}^+(o)\hat{O}(\tau)\right\rangle}
\tag{5.16}
$$

$\left\langle\hat{O}^+(o)\hat{O}(\tau)\right\rangle$ as thermal average is the van Hove correlation function, known from inelastic neutron scattering, weighted by a geometrical factor from the curly bracket in (5.13). This factor is determined by the nature of the magnetic interaction in the sample as discussed in chapter 3. As an example consider a polycrystal or a crystal with cubic symmetry. Then the average over muon polarisation with respect to the crystal axises gives

$$
\begin{aligned}
\overline{\xi\eta} = \overline{\xi\zeta} = \overline{\zeta\eta} &\quad all = 0\\
\overline{\xi\xi} = \overline{\eta\eta} = \overline{\zeta\zeta} &\quad = 2/3
\end{aligned}
$$

Then the relaxation rate is just the Fourier transform of the correlation function of the fluctuating magnetic field at the site of the implanted muon.

$$
\boxed{\lambda = 2W = \frac{1}{3}\left(g\frac{\mu_\mu}{\hbar}\right)^2\int_{-\infty}^{+\infty} d\tau e^{-i\omega_\mu\tau}\left\langle\vec{B}(0)\vec{B}(\tau)\right\rangle}
\tag{5.17}
$$

We shall see that this kind of correlation functions will also be addressed by inelastic neutron scattering. Furthermore the information we can extract from μSR-experiments has very much in common with what we may learn from NMR-experiments (nuclear magnetic resonance).

An advantage of μSR is that by the observation of the direct decay signal no rf-field is needed in order to observe the precession. Due to the skin-effect an rf-field may not penetrate into the bulk of certain kind of samples (e.g. superconductors).

On the other side the question about the stopping site of the muon remains sometimes as an uncertainty. With some additional experimental effects this question can often be answered. The electric charge of the muon, giving rise to a local lattice distortion (expressed by $\eta(\vec{x})$ in (3.8)) may cause some uncertainty in the interpretation of the data.

VI. Low Energy – MuSR [5]

While the muon charge may – as just mentioned – cause some complications, it opens up on the other hand a great opportunity to the experimental control of the beam. By means of electrostatic lenses we can achieve a geometrical control of the beam spot on the sample. Furthermore by control of the beam energy we may determine the penetration depth of the muons into the sample.

Fig. 6 shows the set-up of such a facility. The muon originates from the surface of a primary target with muon energy around 4 MeV. The muon polarization is practically 100%. In a moderator cell consisting of solid N_2 or Ar the muons are slowed down to an energy of approximately E~15 eV (Fig. 7). Thereby the polarization is conserved. This low energy beam is then reflected by ninety degrees on an electro static mirror. The resulting muons with now transverse polarization are then guided by means of an electrostatic lense system towards the sample. The sample containment is electrostatically biased (± 12.5 keV) and the extraction potential at the moderator is 12-20 keV. This allows for an implantation energy of the muons within the range of 0.5 – 30 keV in order to control the penetration depth into the sample. The whole system is in a UHV of 10^{-9} – 10^{-10} mbar. Let us finally show an example of a profile measurement using this facility.

It is well known that a superconductor, apart from showing zero resistivity, is also an ideal diamagnet. That is, below transition temperature a magnetic field is ejected from the sample (Meissner-effect) [6]. Indeed the London equation

$$\vec{J}(\vec{x}) = -\frac{e^2 n}{mc}\vec{A}(\vec{x}) \tag{6.1}$$

relating the current and the vector potential of the magnetic field yields – with Maxwells equations – the magnetic field dependence (Fig. 8)

$$\vec{B} = \vec{B}_0 e^{-3/\lambda} \tag{6.2}$$

with a penetration depth

$$\lambda = \sqrt{\frac{mc^2}{\omega\pi n e^2}} \tag{6.3}$$

This assumes that the superconducting wave function is unaffected by the magnetic field.

However, we also know that the superconductive state is destroyed by the application of a sufficiently high field B_c. To gain some insight we write the Fourier-transform of a generalized (6.1) as

$$\vec{J}_{\vec{q}} \sim \Gamma(\vec{q})\vec{A}(\vec{q}) \tag{6.4}$$

$\Gamma(\vec{q})$ = const. corresponds to $\Gamma(\vec{x}) \sim \delta(o)$ and leads directly to the London equation (6.1). Large $\vec{q}$'s involve however large energies and hence to destruction of the Cooper pairs. Therefore $\Gamma(\vec{q}) \to 0$ for large $q >> q_c$, where q_c is the correlation length (actually the size of the Cooper pairs). The relation (6.1) has then to be replaced by

$$\vec{J}(\vec{x}) = \int \Gamma(\vec{x}-\vec{x}')\vec{A}(\vec{x}')d^3x' \tag{6.5}$$

hence a non-local relation. This then leads to a penetration law of the magnetic field which is **not** exponential.

Penetration controlled μSR offers now the experimental method to investigate this situation as is demonstrated in Fig. 9.

Table I:

Property	**Values**
Mass (m_μ)	206.768 m_c = 0.1126 m_p = 105.6595 MeV/c^2
Charge	+e, -e
Spin	$\frac{1}{2}\hbar$
Magnetic Moment (μ_μ) (in units μ_p)	3.1833
Gyromagnetic Ratio $\gamma_\mu / 2\pi$	13.5539 kHz G^{-1}
g-factor	2.0023
Lifetime	2.1970 μs

References:

[1] Quarks and Leptons
F. Halzer, A.d. Martin,
John Wiley and Sons, 1984

[2] A. Schenck
Muon Spin Rotation Spectroscopy (Adam Hilger, Bristol), 1985
A. Schenck, F.N. Gygax
Handbook of Magnetic Materials
Vol. 9, Edit. K.H.J. Buschkow, Elsevier 1995

[3] Ch. P. Slichter
Principles of Magnetic Resonance
Harper and Row 1963

[4] S.W. Lovesey, E. Balcar, A. Cuccoli
J. Phys.: Condens. Matter **7** (1995) 2615-2631

[5] E. Morenzoni et al.
Nucl. Instr. and Methods in Phys. Research B 192 (2002) 254-266

[6] Principles of the Theory of Solids
J.M. Ziman, Cambridge University Press 1964, Solid State Physics,
N.W. Ashcroft, N.D. Mermin, Saunders College Publish. 1975

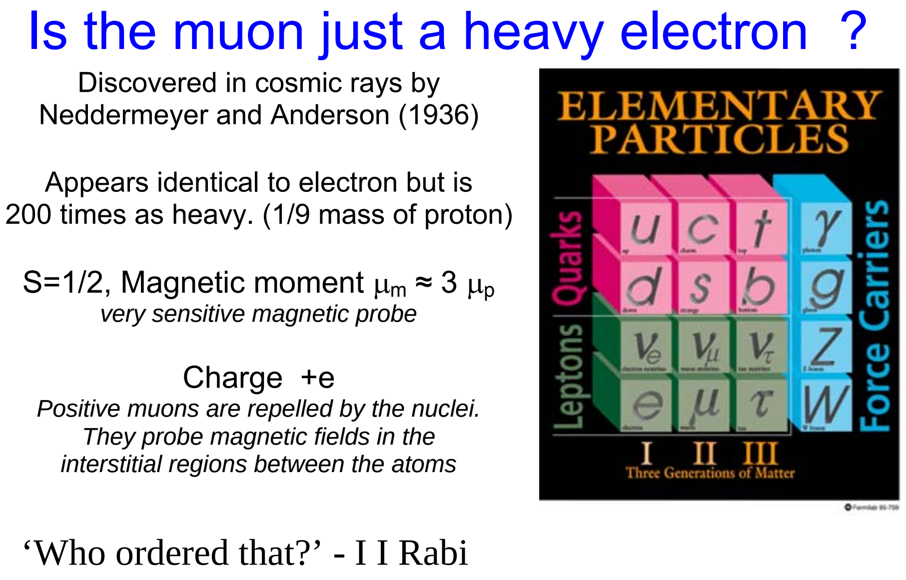

Figure 1: the position of the muon within the scheme of the standard model of elementary particles

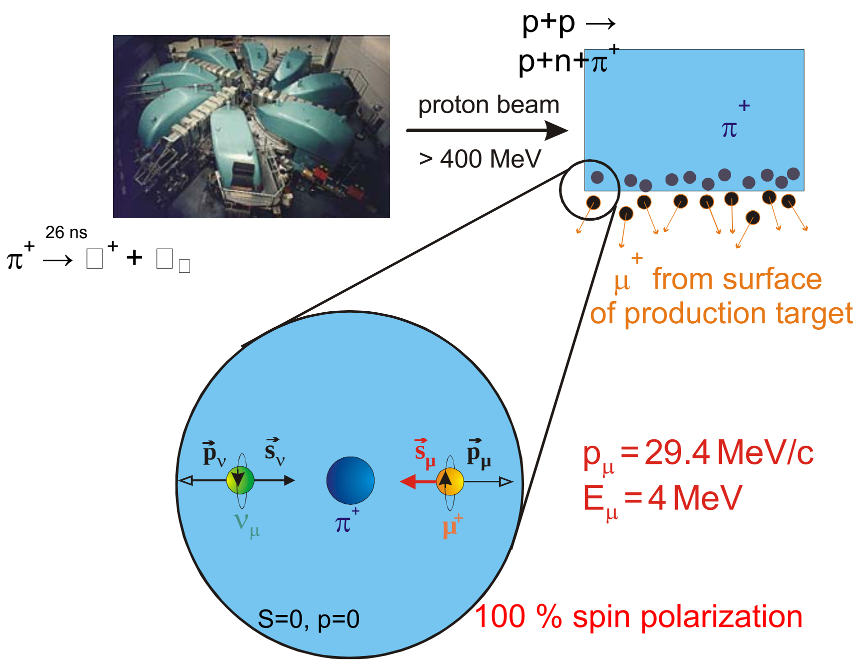

Figure 2: Penetration of π-mesons and their decay

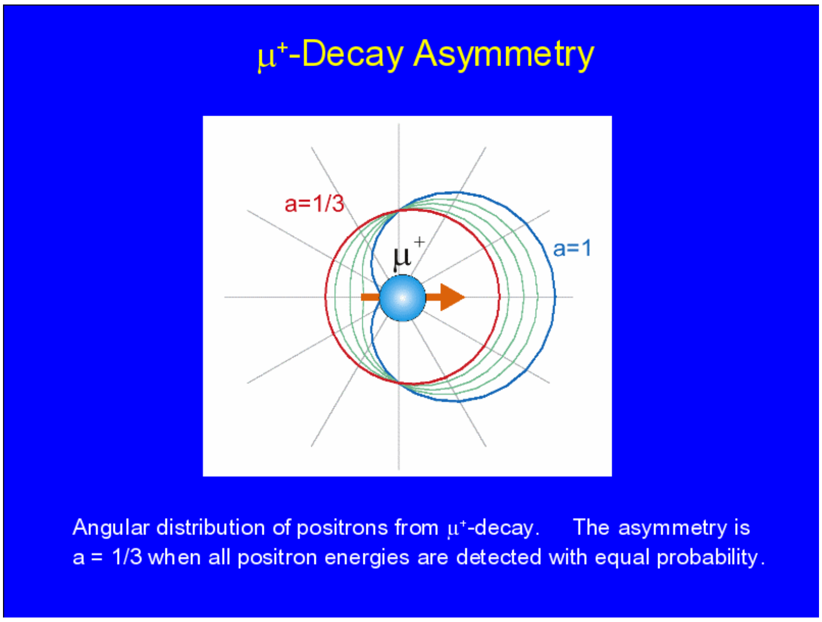

http://musr.triumf.ca/intro/musr/muSRBrochure.pdf by Jeff E. Sonier

Figure 3: The asymmetry of positron from μ^+-decay

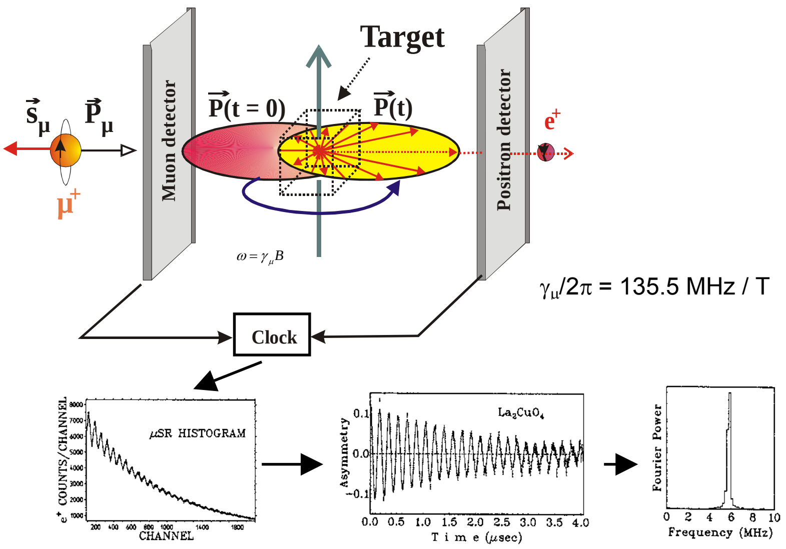

Figure 4: The basic principle of a μSR-experimental. The signals are explained in the test.

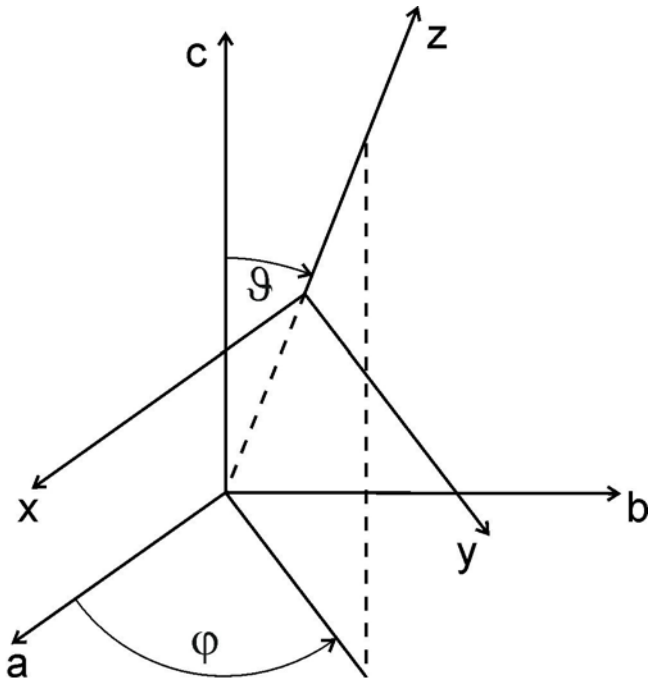

Figure 5: Crystal axises (a,b,c) and the magnetic system (x,y,z) with the corresponding rotation angles

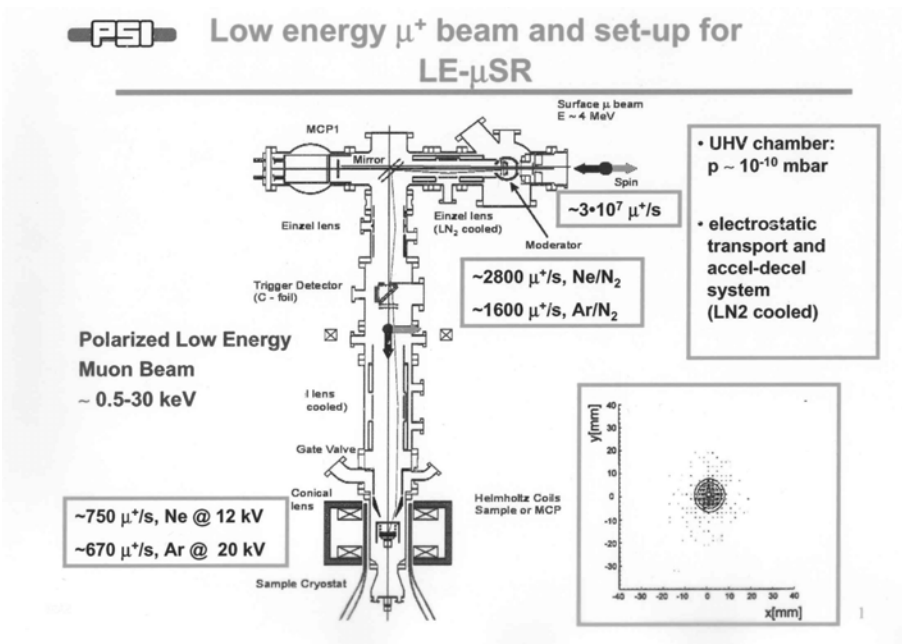

Figure 6: Lay-out of a low energy μSR-experiment with control of the penetration depth

Muon moderation (E. Morenzoni et al.)

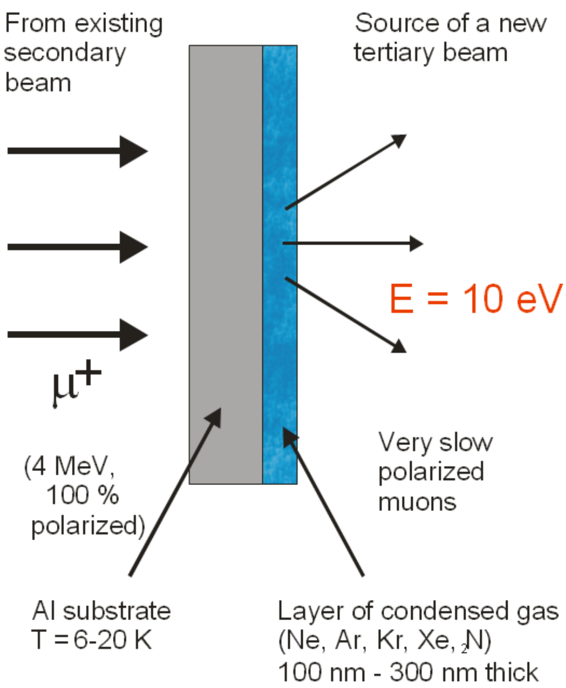

Figure 7: Principle of a muon moderator

Direct measurement of the London Penetration Depth

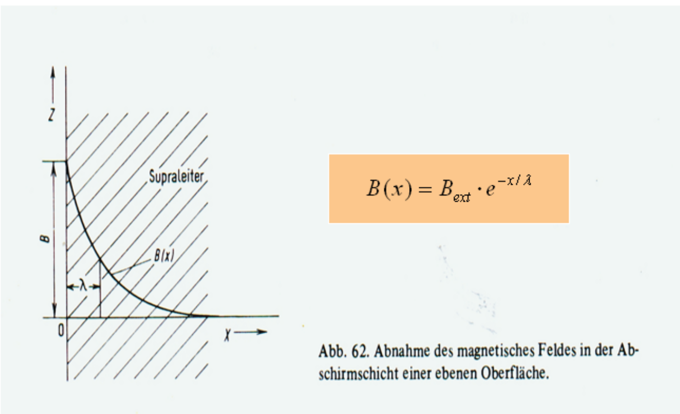

aus:
W. Buckel: "Supraleitung" Grundlagen und Anwendungen

A magnetic field B(z) penetrates into a superconductor on a typical length scale, the London penetration depth λ

Figure 8: The London penetration in the context of the Meissner effect

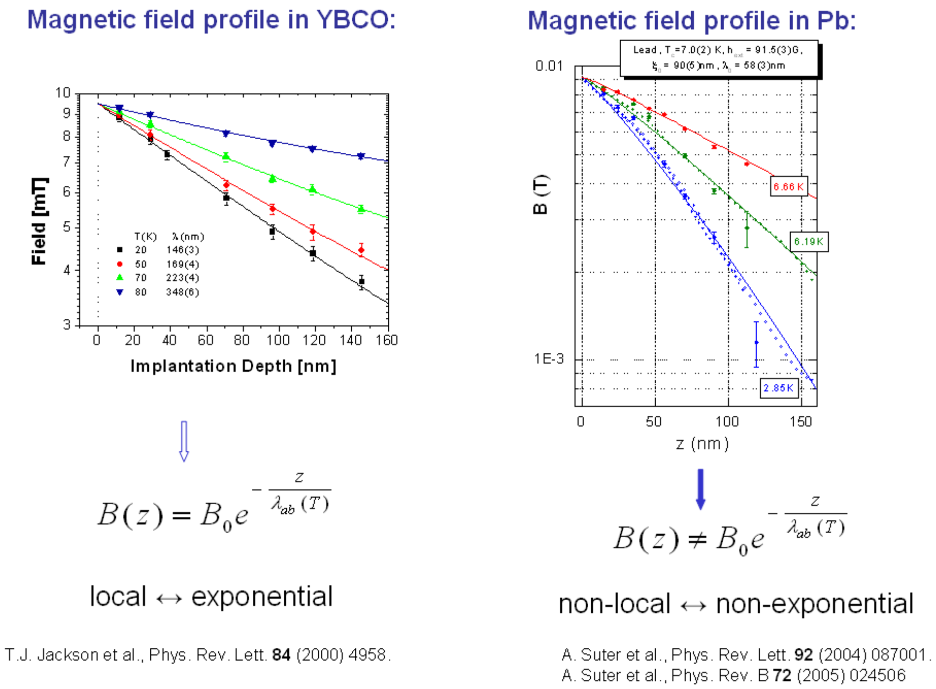

Figure 9: Experimentally determined field profiles into two different samples. A local and a non-local case are shown.